The Influence of Horizontal Reinforcement on Punching Shear Strength

Ali N. Ameen

Department of Civil Engineering, College of Engineering, University of Baghdad, Baghdad, Iraq
ali.nihad2101m@coeng.uobaghdad.edu.iq (corresponding author)

Mohannad H. Al-Sherrawi

Department of Civil Engineering, College of Engineering, University of Baghdad, Baghdad, Iraq
dr.mohannad.al-sherrawi@coeng.uobaghdad.edu.iq

ABSTRACT

The slab is more petite and space-efficient in flat plate buildings since it is supported directly by columns rather than beams or drop panels, allowing additional floors to be added. Despite these benefits, a flat plate slab is vulnerable to brittle punching shear, a catastrophic collapse caused by the abrupt propulsion of a slab piece out from underneath by a column. In this study, Finite Element Analysis (FEA) was provided and carried out in ABAQUS/CAE 2019 to model the effects of punching shear impact on a flat plate reinforced with horizontal steel bars that vary in position, diameter, and number. Concrete was represented in the model by 8-noded hexahedral 3D brick elements and steel reinforcements by 2-noded linear 2D beam elements. The model has been modified according to the results of the experiments. In order to determine how different quantities and sizes of horizontal steel bars placed at different locations in a flat plate affected the slab's performance, parametric analysis was conducted. According to the outcomes, the shear capacity increases between 0.37 and 9.85% as the diameter of bars increases, between 1.2 and 22.9% as the quantity of bars increases, and between 1.99 and 26.1% as the bars shift from the tension side to the compression side.

Keywords-flat plates; punching shear; reinforced concrete; horizontal reinforcement; finite element analysis

I. INTRODUCTION

The flat plates experience an unanticipated failure due to punching shear, which can have disastrous repercussions [1, 2]. Several parameters affect the punching shear of flat plates. These include shear and flexural reinforcement, boundary conditions, concrete strength, column-to-slab ratio, and the presence or absence of apertures [3-5]. There are several ways in which design codes deal with the issue of punching failure. Unlike the European standard Euro-Code2 [6], the American standard ACI 318-19 [7] disregards the effects of horizontal reinforcement. According to the design code, the critical punching zone could be half or double of the effective slab depth measured from the column surface. A flexural punching mechanism that develops due to local flexural yielding all over the column might lead to failure [8]. Authors in [9] proposed bracing the area around the columns with bent bars and stirrups to prevent brittle punching failure. Authors in [10] examined the effect of the ratio of horizontal flexural reinforcing bars, the number of stirrups, their breadth, and the spacing between them on seven flat slabs subjected to punched shear. Non-linear finite element models were presented in [11] to study flat slab punching shear behavior and the effects of concrete's compressive strength, steel yield strength, and flexural reinforcement. The findings of six experimental square concrete flat plates reinforced with steel collars were discussed in [12, 13]. Authors in [14] used Z-shape shear reinforcement to stiffen flat plates in a non-linear Finite Element Analysis (FEA). Five slab-column connections without shear reinforcement were investigated in [15] deploying the concrete damage plasticity model.

II. DESCRIPTION OF THE EXPERIMENTAL CONTROL SLAB

The provided model was validated utilizing an evaluated experimental sample [14]. Figure 1 shows the dimensions, boundary conditions, and reinforcement specifics. Table I summarizes the characteristics of the steel bars and the concrete rebar.

TABLE I.   MATERIAL CHARACTERISTICS OF THE CONTROL SLAB

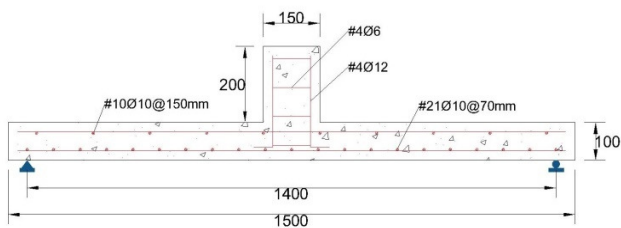| Concrete's compressive strength [MPa]	Concrete's tensile strength [MPa]	Steel's yield strength [MPa]	Column's steel yield strength [MPa]	Yield strength of stirrups [MPa]
35	3.8	470	455	610

Fig. 1.   Reinforcement details of the control slab.

III. SIMULATION OF THE SLAB NUMERICAL MODEL

Using ABAQUS/CAE 2019 [15], a FEA numerical model was developed to simulate the selected slab sample. The model keeps spans from the experimental test. The symmetry of the geometry, boundary conditions, and loading mechanism [16] were considered while modeling a quarter of the flat-plate slab in ABAQUS/CAE 2019. The internal surfaces have symmetry requirements applied, as evidenced in Figure 2. A controlled linear displacement up to a maximum of 20 mm was applied to the column's top surface during the quasi-static dynamic/implicit test. The Concrete Damage Plasticity model developed by ABAQUS/CAE 2019 was used. This model [17] based on criteria established in [18], states that crushing and cracking are the two main ways concrete fails. The magnitude of the variables used for the Concrete Damage Plasticity characteristics is depicted in Table II.
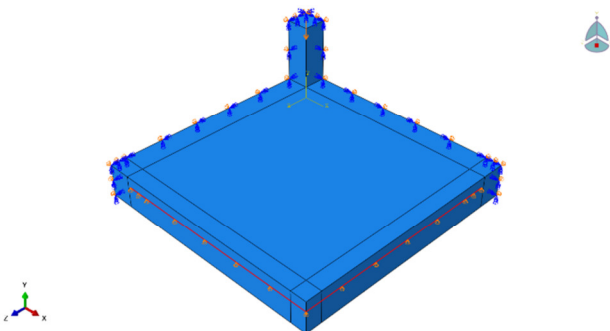

Fig. 2.   Geometry and supports of the control slab.

The application of von Misses failure criteria to the steel rebar was carried out on the assumption of perfect bonding between the concrete and steel surfaces. C3D8R, an 8-noded hexahedral element with reduced integration, was used for the concrete. The steel component, on the other hand, is a 2-node space linear beam (B31). After extensive testing with various mesh sizes, it was determined that the 20 mm mesh produced the most precise outcomes.

TABLE II.   CONCRETE DAMAGE PLASTICITY PROPERTIES

Dilation angle ψ	Eccentricity ε	Shape parameter Kc	Max. compression axial/biaxial	Viscosity μ
42	0.1	1.16	0.667	0.00002

IV. VERIFICATION OF CALIBRATION FOR THE SLAB MODEL

This study compares the load-deflection curves from the experimental test done [14] with the slab model simulated by ABAQUS/CAE 2019. With S0 acting as the control sample, the comparison is illustrated in Figure 3 and Table III.
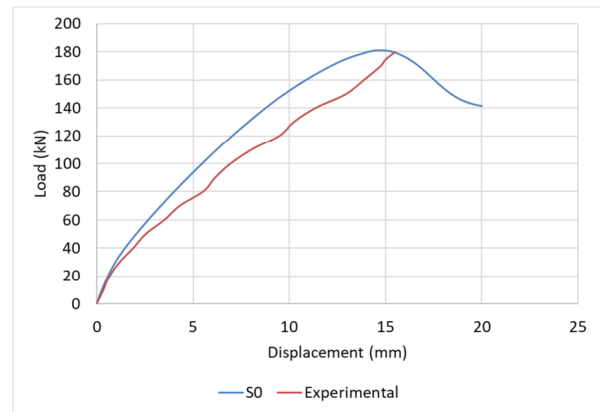

Fig. 3.   Load-deflection relationship of the control slab.

Table III demonstrates that the study follows the results of the tests conducted in [14]. Due to the ideal conditions suggested by the finite element model, including a homogeneous material, no shrinkage, and no slide between reinforcing bars and concrete, all numerical curves were stiffer and more regular than the actual curves. Both the ultimate load and deflection had relative inaccuracies of 0.561% and 6.129%, respectively.

TABLE III.   COMPARISON BETWEEN THE EXPERIMENTAL AND THE FEA OUTCOMES OF CONTROL FLAT-PLATE

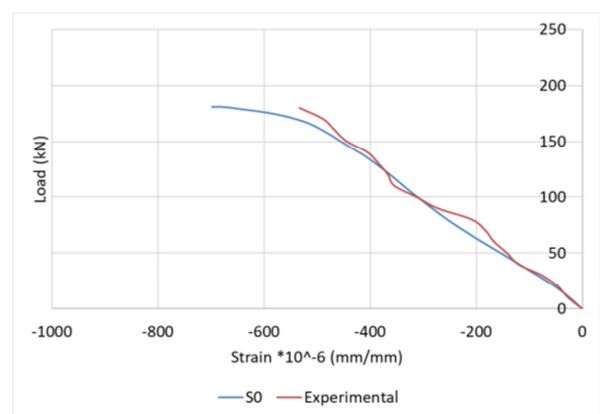| Specimen ID	Ultimate load (kN)		Ultimate deflection (mm)		The discrepancy of Pu (%)
	Exp	FEA	Exp	FEA	
S0	180	181.01	15.5	14.55	0.561%

Fig. 4.   Load-strain curves of the concrete of the control slab.

Figures 4 and 5 portray the load-strain curves for concrete and steel derived from the experimental test conducted in [14], compared to the slab model proposed in this study.

Measurements of the load-strain curve for both the concrete and the steel were taken during the experimental and the numerical tests at a distance of (d/2) from the column's surface, on the compression side for the former and the tension side for the latter. A strong agreement between the experimental testing and finite element analysis can be seen.

Calibrations were carried out using both quantitative and qualitative methods. Figure 6 displays the results of the numerical and experimental analyses of the cracking pattern.
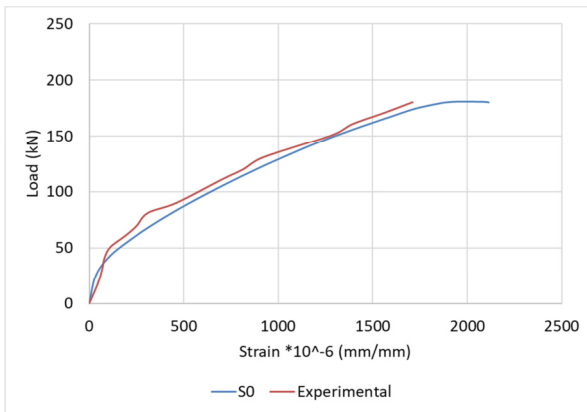
Fig. 5.   Load-strain curves of the steel of the control slab.
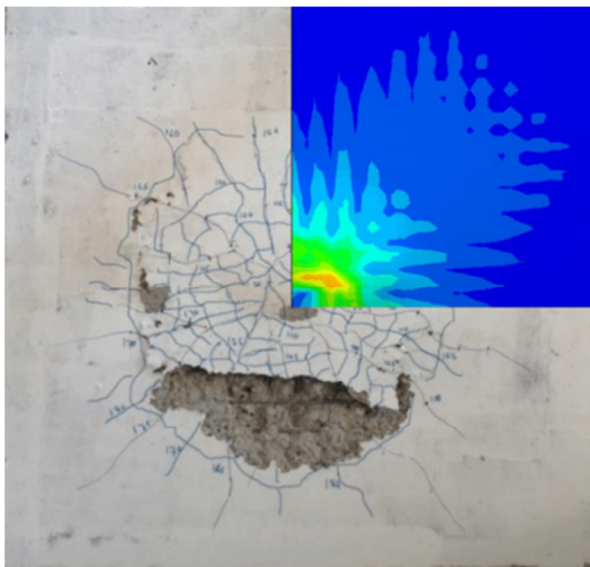
Fig. 6.   Experimental and FEA crack patterns of the control slab.

V.   PARAMETRIC STUDY AND RESULTS

Eleven reinforced concrete slabs were classified into three groups (horizontal steel bar diameters, bar numbers, and bar position). Group one specimens (S1, S2, S3, S4, and S5) were reinforced with two-way horizontal steel bars of 12, 16, 20, 25, and 36 mm diameter. All specimens consisted of two bars placed in the slab. Group two (S4, S6, S7, S8, and S9) consisted of specimens reinforced with two-way horizontal steel bars using 1, 2, 3, 4, and 5 bars with 25 mm diameter. Group three (S4, S10, and S11) used two-way reinforcement

bars in various locations (middle of the slab, with flexural tension and compression reinforcement). The specimens consisted of 2 bars with 25 mm diameter. The development length of the additional bars was 750 (375 for the quarter model). Figure 7 illustrates where the extra bars were located.
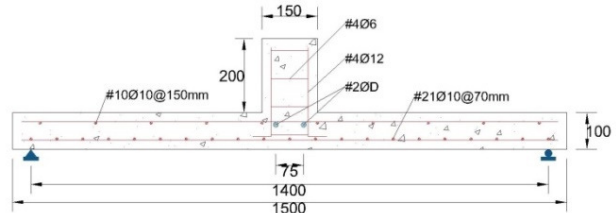

Fig. 7.   Method of strengthening the specimen.

Three categories were employed in the discussions of the findings to understand flat-plate structural behavior better. These are:

1. Pattern of cracks and failure mode.

2. Load-deflection behavior with ultimate load.

3. Displacement stages and displacement along the slab.

A. Pattern of Cracks and Failure Mode

Brittle failure was observed in every slab that was tested. Every specimen showed the same punching shear angular cracking around the column. The cracking patterns of Group 1 are manifested in Figures 8–12. The cracks are more evenly spread with an increasing diameter, improving resistance. Similarly, for slabs S6–S10, the cracks are more evenly distributed with the increasing number of horizontal bars, which implies a rise in the slabs' punching shear capacity. Group 2's crack patterns can be seen in Figures 11 and 13–16. Figures 11, 17, and 18 exhibit the crack patterns of Group 3. Group 3's crack patterns show that the cracks are getting reduced and distributed more as the installed steel moves from the tension side to the compression side. The mode of failure of all the groups was pure punching shear, because the concrete and steel did not reach the yield state (at strain of 2350×10^{-6}).
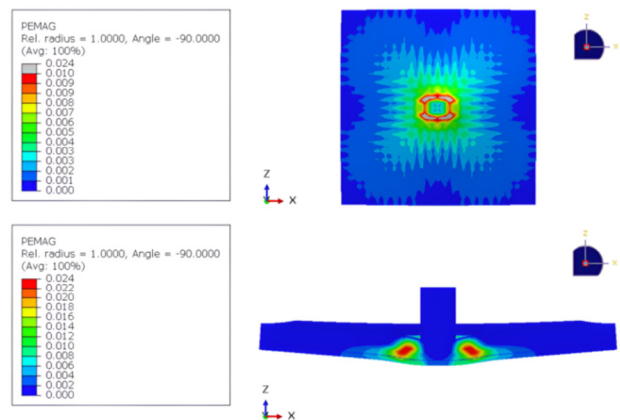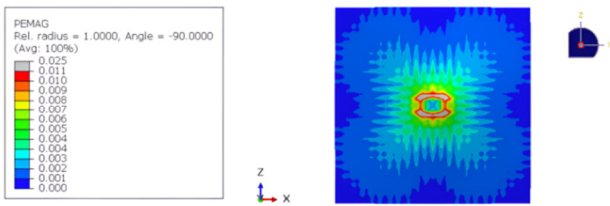

Fig. 8.   Crack progression of S1.
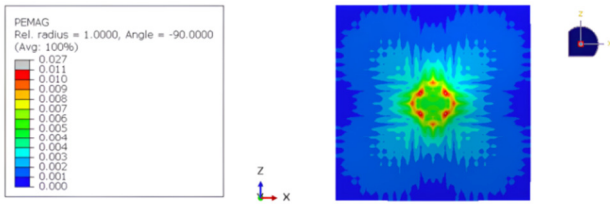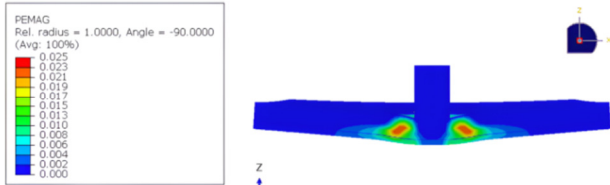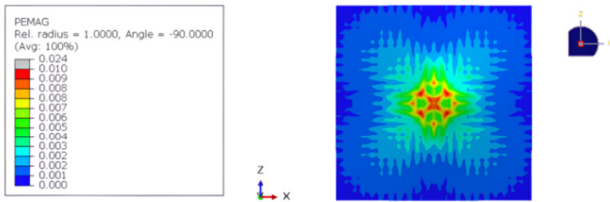
Fig. 9.   Crack progression of S2.

Fig. 10.   Crack progression of S3.
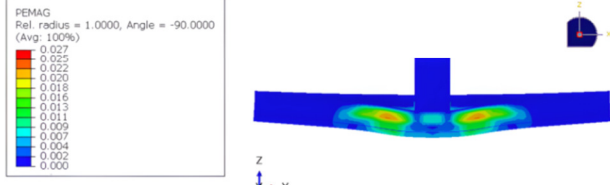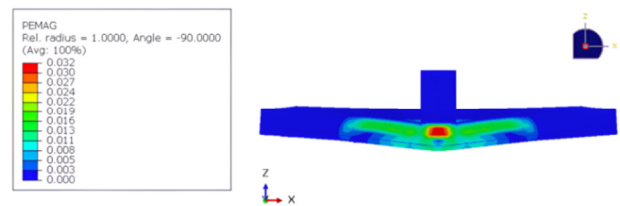

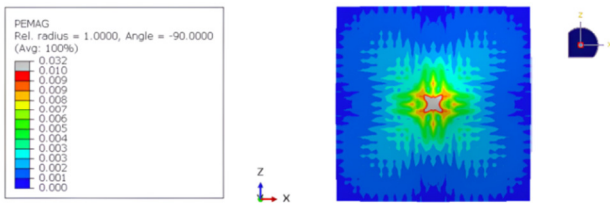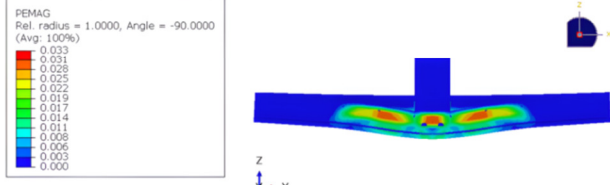Fig. 11.   Crack progression of S4.

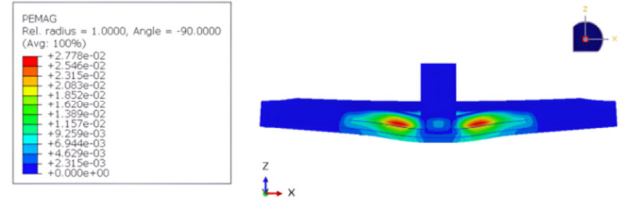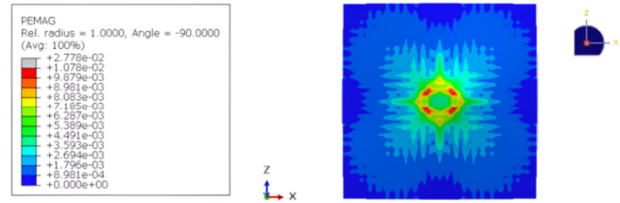Fig. 12.   Crack progression of S5.

Fig. 13.   Crack progression of S6.
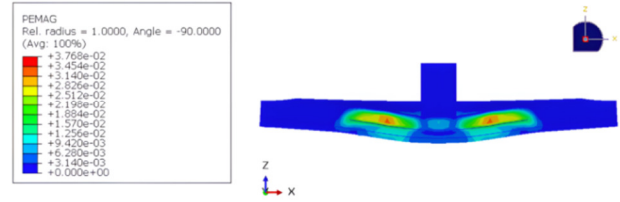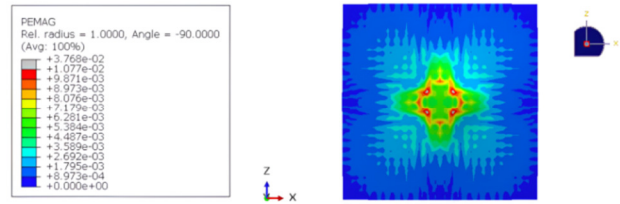

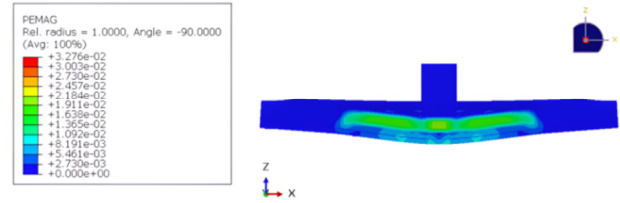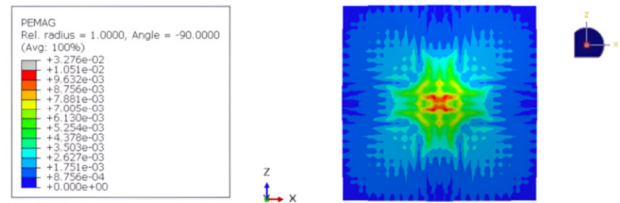Fig. 14.   Crack progression of S7.

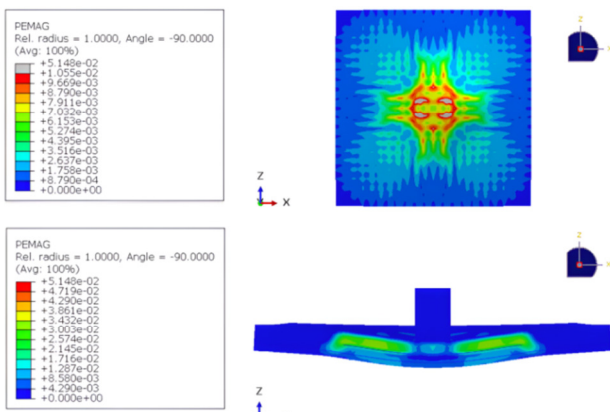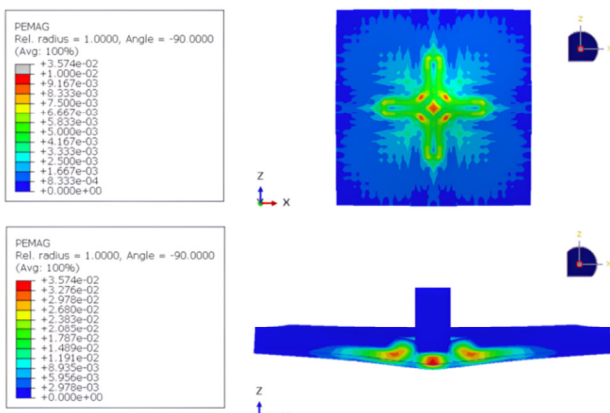Fig. 15.   Crack progression of S8.

Fig. 16.   Crack progression of S9.

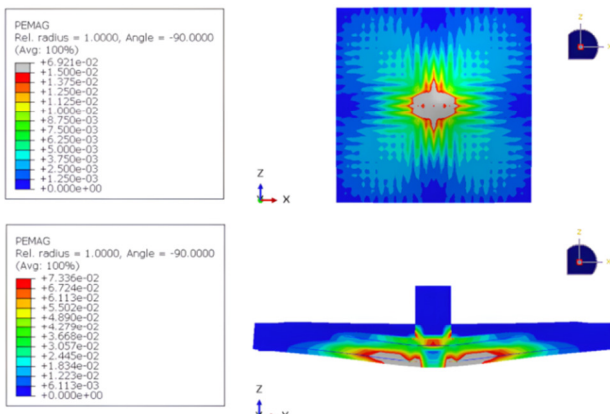Fig. 17.   Crack progression of S10.

Fig. 18.   Crack progression of S11.

B. Load-Deflection Behavior with Displacement Stages, Ultimate Load, and Displacement along the Slab

Vertical displacement was computed at the middle span for each static test load increment and specimen. P_{cr} represents the load of the first cracking. The control specimen had a P_{cr} value of 41.44 kN, and the addition of extra bars resulted in an improvement of less than 0.01 kN for all specimens. This improvement was not deemed significant, thus, it was

disregarded, except for S12, in which it was 49.44 kN because the initial crack was formed at the tension side of the flat-plate, where the inserted steel bars were located. In contrast, the additional bars for the other specimens were located in the middle of the slab. Figures 19-21 demonstrate how diameter, number, and bar position affect the load-deflection behavior at the slab center. Each slab is compared to S0.
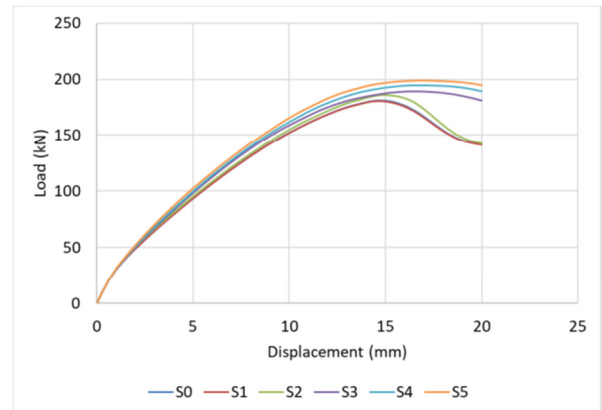

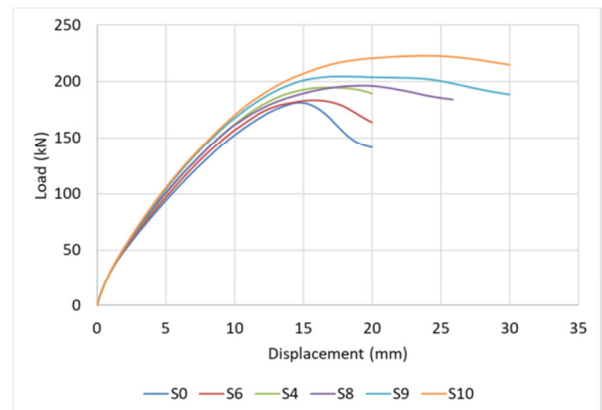Fig. 19.   Load-deflection curves of Group 1.

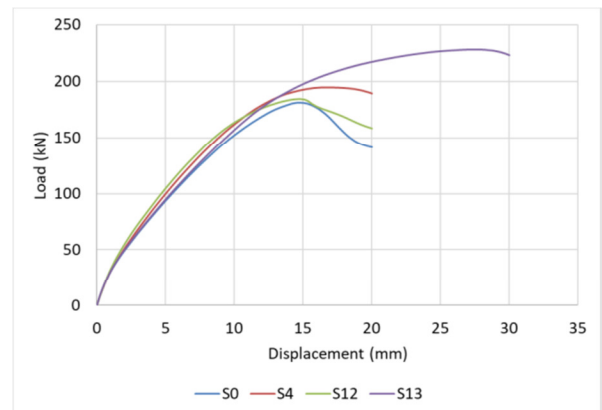Fig. 20.   Load-deflection curves of Group 2.

Fig. 21.   Load-deflection curves of Group 3.

Adding 12 mm diameter bars does not enhance load-deflection characteristics, however, increasing the diameter

improves flat-plate punching shear strength by a slight amount. Inserting one 25 mm bar at the center of the slab improves punching shear strength, and adding more bars increases the capacity further. Group 3 shows that inserting the bar at the tension side of the slab improves stiffness. However, it slightly increases the bearing load, while inserting the bar toward the compression side lowers stiffness and increases bearing load. Inserting the bar on the compression side improves the load-deflection behavior.
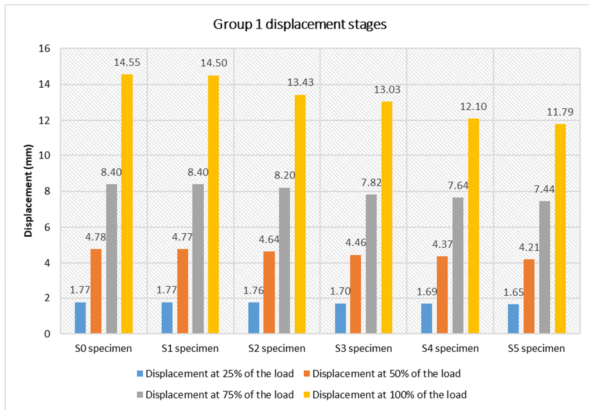

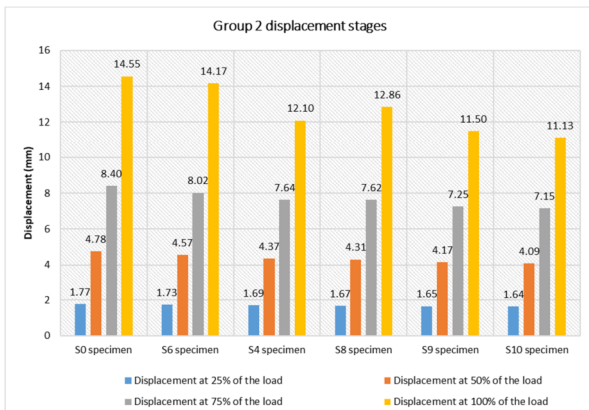Fig. 22.   Displacement stages of Group 1.

Fig. 23.   Displacement stages of Group 2.
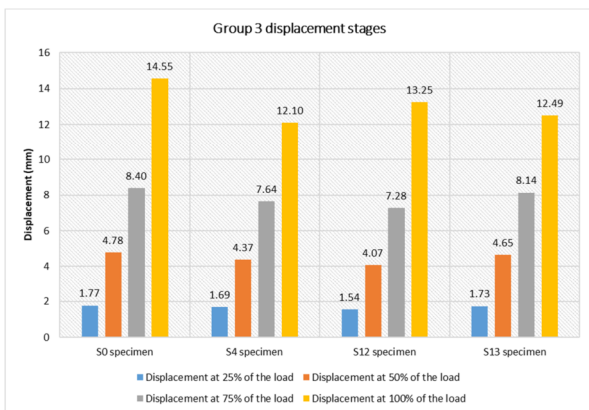

Fig. 24.   Displacement stages of Group 3.

Figures 22-24 display the first, second, and third groups' displacement during all load phases. The deflection reduces as bar diameter, number, and slab position move from tension to compression. Table IV depicts each specimen's final load and improvement.

TABLE IV.   ULTIMATE LOAD AND IMPROVEMENT PERCENTAGE

Specimen ID	Ultimate load (kN)	Improvement (%)
S1	181.69	0.37 %
S2	186.19	2.86 %
S3	189.42	4.64 %
S4	194.68	7.55 %
S5	198.85	9.85 %
S6	183.24	1.23 %
S7	196.31	8.45 %
S8	204.46	12.95 %
S9	222.55	22.94 %
S10	184.63	1.99 %
S11	228.37	26.16 %

VI.   CONCLUSIONS

An existed experimental test was modeled as a reference specimen in ABAQUS software. Eleven numerical models of flat plates were used to show the effect of horizontal steel bars on the punching shear capacity. These models were classified in three groups to demonstrate the effect of each considered perimeter (diameter, number, and location of bars). The results exhibit good improvement, especially when the flat-plate was reinforced using five steel bars and when the additional bars were located at the compression side, which had a huge impact on punching shear capacity. The main conclusions from the results of this study are:

- The punching capacity of flat-plate slabs is increased when they are reinforced with horizontal bars, which is an easy, adaptable, and economical method.

- The slabs' punching shear capacity was improved as the bar diameter increased. The bearing load rose by 0.37, 2.86, 4.64, 7.55, and 9.85% for diameters of 12, 16, 20, 25, and 36 mm, respectively.

- Higher punching shear capacity was achieved with higher bar quantity. The bearing load rose by 1.53, 7.55, 8.45, 12.95, and 22.94% as the bar number grew from 1 to 5.

- Inserting the bars at the slab's tension side increased its stiffness, but the maximum shear capacity reveals an unnoticeable improvement of 1.99 %.

- Shifting the bars from the tension side to the compression side made the slab less stiff and increased the maximum shear capacity. By placing the horizontal bars in the middle of the slab, the shear capacity increased by 7.55%, whereas placing the bars at the compression side gave the best improvement of 26.16%.

REFERENCES

[1] J. Moe, *Shearing strength of reinforced concrete slabs and footings under concentrated loads*. Washington, DC, USA: Portland Cement Association, 1961.

[2] S. King and N. J. Delatte, "Collapse of 2000 Commonwealth Avenue: Punching Shear Case Study," *Journal of Performance of Constructed Facilities*, vol. 18, no. 1, pp. 54–61, Feb. 2004, https://doi.org/10.1061/(ASCE)0887-3828(2004)18:1(54).

[3] A. H. H. Al-Shammari, "Effect of openiings with or without strenghening on punching shear strength for reinforced concrete flat plates," *Journal of Engineering*, vol. 17, no. 2, pp. 218–234, Apr. 2011, https://doi.org/10.31026/j.eng.2011.02.03.

[4] M. A. Golham and A. H. A. Al-Ahmed, "Strengthening of GFRP Reinforced Concrete Slabs with Openings," *Journal of Engineering*, vol. 30, no. 1, pp. 157–172, Jan. 2024, https://doi.org/10.31026/j.eng.2024.01.10.

[5] Nazar K. Oukaili and T. S. Salman, "Punching Shear Strength of Reinforced Concrete Flat Plates with Openings," *Journal of Engineering*, vol. 20, no. 1, pp. 1–20, Jan. 2014, https://doi.org/10.31026/j.eng.2014.01.01.

[6] *ACI 318-19(2019), Building Code Requirements for Structural Concrete and Commentary*. Farmington Hills, MI, USA: ACI Concrete, 2019.

[7] *BS EN 1992-1-1 (2004), Eurocode 2: Design of concrete structures - Part 1-1: General rules and rules for buildings*. London, UK: British Standards Institution, 2004.

[8] A. M. Hameed, H. M. Husain, and M. H. Al-Sherraw, "Analysis of Corner Column-Slab Connections in Concrete Flat Plates," *East African Scholars Journal of Engineering and Computer Sciences*, vol. 2, no. 1, pp. 37–46, 2019.

[9] C. E. Broms, "Concrete flat slabs and footings: Design method for punching and detailing for ductility," Ph.D. dissertation, Royal Institute of Technology, Stockholm, Sweden, 2005.

[10] R. T. S. Mabrouk, A. Bakr, and H. Abdalla, "Effect of flexural and shear reinforcement on the punching behavior of reinforced concrete flat slabs," *Alexandria Engineering Journal*, vol. 56, no. 4, pp. 591–599, Dec. 2017, https://doi.org/10.1016/j.aej.2017.05.019.

[11] M. Navarro, S. Ivorra, and F. B. Varona, "Parametric computational analysis for punching shear in RC slabs," *Engineering Structures*, vol. 165, pp. 254–263, Jun. 2018, https://doi.org/10.1016/j.engstruct.2018.03.035.

[12] A. A. Abdulhussein and M. H. Al-Sherrawi, "Experimental study on strengthening punching shear in concrete flat plates by steel collars," *AIP Conference Proceedings*, vol. 2651, no. 1, Mar. 2023, Art. no. 020026, https://doi.org/10.1063/5.0130802.

[13] A. A. Abdulhussein and M. H. Al-Sherrawi, "Experimental and Numerical Analysis of the Punching Shear Resistance Strengthening of Concrete Flat Plates by Steel Collars," *Engineering, Technology & Applied Science Research*, vol. 11, no. 6, pp. 7853–7860, Dec. 2021, https://doi.org/10.48084/etasr.4497.

[14] A. M. Abbas, H. K. Hussain, and A. S. Saadoon, "Non-linear analysis to improve punching shear strength in flat slab using z-shape shear reinforcement," *Muthanna Journal of Engineering and Technology*, vol. 7, no. 1, pp. 65–70, Jun. 2019, https://doi.org/10.52113/3/mjet/2019-7-1/65-70.

[15] A. S. Genikomsou and M. A. Polak, "Finite element analysis of punching shear of concrete slabs using damaged plasticity model in ABAQUS," *Engineering Structures*, vol. 98, pp. 38–48, Sep. 2015, https://doi.org/10.1016/j.engstruct.2015.04.016.

[16] A. N. Dalaf and S. D. Mohammed, "The Impact of Hybrid Fibers on Punching Shear Strength of Concrete Flat Plates Exposed to Fire," *Engineering, Technology & Applied Science Research*, vol. 11, no. 4, pp. 7452–7457, Aug. 2021, https://doi.org/10.48084/etasr.4314.

[17] *ABAQUS/CAE User's Manual*. Karlsson & Sorensen, 2002.

[18] G. A. Almashhadani and M. H. Al-Sherrawi, "Effect Change Concrete Slab Layer Thickness on Rigid Pavement," *Engineering, Technology & Applied Science Research*, vol. 12, no. 6, pp. 9661–9664, Dec. 2022, https://doi.org/10.48084/etasr.5283.

[19] D. C. Drucker and W. Prager, "Soil Mechanics and Plastic Analysis or Limit Design," *Quarterly of Applied Mathematics*, vol. 10, no. 2, pp. 157–165, 1952, https://doi.org/10.1090/qam/48291.

[20] J. Lubliner, J. Oliver, S. Oller, and E. Oñate, "A plastic-damage model for concrete," *International Journal of Solids and Structures*, vol. 25, no. 3, pp. 299–326, Jan. 1989, https://doi.org/10.1016/0020-7683(89)90050-4.